

## Prenatal hypoxia produces memory deficits associated with impairment of long-term synaptic plasticity in young rats

Igor A. Zhuravin<sup>a</sup>, Nadezhda M. Dubrovskaya<sup>a</sup>, Dmitry S. Vasilev<sup>a</sup>, Tatyana Yu. Postnikova<sup>a</sup>, Aleksey V. Zaitsev<sup>a,b,\*</sup>

<sup>a</sup> Sechenov Institute of Evolutionary Physiology and Biochemistry of RAS (IEPhB), 44, Toreza pr., Saint Petersburg 194223, Russia

<sup>b</sup> Institute of Experimental Medicine, Almazov National Medical Research Centre, 2 Akkuratova Street, Saint Petersburg 197341, Russia

### ARTICLE INFO

#### Keywords:

Prenatal hypoxia  
LTP  
Synaptopodin  
NMDA receptor  
Learning  
Novel object recognition

### ABSTRACT

Prenatal hypoxia often results in dramatic alterations in developmental profiles and behavioral characteristics, including learning and memory, in later life. Despite the accumulation of considerable amounts of experimental data, the mechanisms underlying developmental deficits caused by prenatal hypoxia remain unclear. In the present study, we investigated whether prenatal hypoxia on embryonic day 14 (E14) affected synaptic properties in the hippocampus and hippocampal-related cognitive functions in young rats. We found that 20- to 30-d-old rats subjected to prenatal hypoxia had significantly disturbed basal synaptic transmission in CA3–CA1 synapses and a two-fold decrease in hippocampal long-term synaptic potentiation. These alterations were accompanied by a significant decline in the protein level of GluN2B but not GluN2A NMDA receptor subunits. In addition, the number of synaptopodin-positive dendritic spines in the CA1 area of the hippocampus was reduced in the rats exposed to prenatal hypoxia. These changes resulted in significant learning and memory deficits in a novel object recognition test.

### 1. Introduction

Prenatal development is a critical period during which the brain structures involved in cognitive functions, including learning and memory, form (Babenko, Kovalchuk, & Metz, 2015; Desplats, 2015). Any disruption during this period can have a significant impact on cognitive functions in later life due to compromised neuronal networking. The latter has been frequently observed in abnormal pregnancies and different animal models exposed to prenatal stress (Barradas et al., 2016; Cai, Xiao, Lee, Paul, & Rhodes, 1999; Desplats, 2015; Nalivaeva, Turner, & Zhuravin, 2018; Vasilev, Dubrovskaya, Tumanova, & Zhuravin, 2016). A number of studies demonstrated that prenatal hypoxia often resulted in dramatic alterations in developmental profiles and behavioral characteristics (Nyakas, Buwalda, & Luiten, 1996; Vasilev et al., 2016). An understanding of the mechanisms of the pathological changes caused by prenatal stress, including hypoxia, is essential for developing new pharmacological and behavioral approaches for attenuation of these developmental abnormalities. Despite the accumulation of considerable amounts of

experimental data, the mechanisms underlying developmental deficits caused by prenatal hypoxia are not fully understood.

Recently, we showed that prenatal hypoxia on embryonic day 14 (E14) and E18 disrupted neuroblast migration, with different outcomes (Vasilev et al., 2016). In the rats subjected to hypoxia on E14, the number of cortical pyramidal neurons and density of labile synaptopodin-positive dendritic spines in the molecular cortical layer decreased during the first month after birth, which affected the development of cortical functions. Other research observed changes in cell morphology in the dorsal hippocampus of hypoxic rats, especially in the CA1, with increased numbers of neurons possessing retracted apical dendrites (Zhuravin, Tumanova, & Vasiliev, 2009).

The hippocampus appears to play a significant role in different cognitive functions, especially memory formation (Bird & Burgess, 2008), and it is highly sensitive to stress (Kim & Diamond, 2002). In terms of cellular mechanisms, hippocampal synaptic plasticity, including long-term potentiation (LTP) and long-term depression (LTD), is considered to underlie certain types of learning and memory (Collingridge, Isaac, & Wang, 2004; Milner, Squire, & Kandel, 1998).

**Abbreviations:** ACSF, artificial cerebrospinal fluid; FV, fiber volley; fEPSP, field excitatory postsynaptic potential; I/O, input/output; LTD, long-term depression; LTP, long-term potentiation; LTM, long-term memory; PPR, paired-pulse ratio; PE, phycoerythrin; PI, preference index; STM, short-term memory; TBS, theta-burst stimulation

\* Corresponding author at: Sechenov Institute of Evolutionary Physiology and Biochemistry of RAS (IEPhB), 44, Toreza pr., Saint Petersburg 194223, Russia.

E-mail address: [aleksey\\_zaitsev@mail.ru](mailto:aleksey_zaitsev@mail.ru) (A.V. Zaitsev).

<https://doi.org/10.1016/j.nlm.2019.107066>

Received 26 March 2019; Received in revised form 31 July 2019; Accepted 6 August 2019

Available online 07 August 2019

1074-7427/ © 2019 Elsevier Inc. All rights reserved.

Therefore, in the present study, we investigated whether prenatal hypoxia on E14 altered hippocampal synaptic plasticity in young rats and led to disturbances in cognitive functions. We also explored some potential molecular and synaptic mechanisms of these disorders.

## 2. Methods

### 2.1. Animals

The study was carried out on 20- to 28-d-old males from the progeny of female Wistar rats of control and experimental (prenatal hypoxia) groups. All animals had access to food and water available ad libitum and were housed under a 12-h light/dark cycle. All experiments were carried out in accordance with the protocol of Sechenov Institute of Evolutionary Physiology and Biochemistry of the Russian Academy of Sciences for the handling of laboratory animals, based on the EU Directive 2010/63/EU for animal experiments.

### 2.2. Model of prenatal normobaric hypoxia

On d 14 of pregnancy, female rats were exposed to normobaric hypoxic hypoxia in a chamber with a capacity of 100 L containing thermoregulation, ventilation, gas analysis, and exhaled CO<sub>2</sub> adsorption systems (Nalivaeva et al., 2018). To create hypoxic conditions, the content of oxygen in the chamber was decreased to 7.0% linearly during the first 10 min by substitution with nitrogen and kept at this level for 3 h. The concentration of CO<sub>2</sub> in the chamber did not exceed 0.2%, and the temperature was maintained at 22 °C. No more than 10 rats were simultaneously placed in the chamber. On d 20 of pregnancy (1 d before giving birth), the females were placed in individual cages. Maternal hypoxia did not affect brood size. On d 2 after birth, only eight pups were left in each brood to minimize the effect of pups nutrition on the processes studied in the experiments.

### 2.3. Hippocampal brain slice preparation

Acute brain slices were prepared as described previously (Plata et al., 2018). Briefly, the rats were decapitated, and their brains were rapidly removed. Horizontal brain slices (400-μm thick) containing the dorsal hippocampus were cut using a vibratome HM 650 V (Microm International, Germany) in ice-cold (0 °C) artificial cerebrospinal fluid (ACSF) composed of (in mM) 126 NaCl, 2.5 KCl, 1.25 NaH<sub>2</sub>PO<sub>4</sub>, 1 MgSO<sub>4</sub>, 2 CaCl<sub>2</sub>, 24 NaHCO<sub>3</sub>, and 10 glucose and then bubbled with carbogen (95% O<sub>2</sub> and 5% CO<sub>2</sub>). The slices were then transferred to oxygenated ACSF and incubated for 1 h at 35 °C before electrophysiological recordings. One to three slices from each rat were used in the experiments.

### 2.4. Field potential recordings

For the electrophysiological study, the hippocampal slices were transferred to a submerged recording chamber, where they were perfused with a constant flow of oxygenated ACSF at a rate of 5 mL/min at room temperature for 15–20 min before the recordings. Two to five slices from each rat were used in the experiment. Extracellular field excitatory postsynaptic potentials (fEPSPs) were recorded from the CA1 stratum radiatum using glass microelectrodes (0.2–1.0 MΩ) filled with ACSF. Synaptic responses were evoked by local extracellular stimulation of the afferent fibers using a twisted nichrome electrode placed in the stratum radiatum at the CA1–CA2 border, approximately 500–700 μm away from the stimulating electrode. At the beginning of each experiment, input/output (I/O) relationships were measured by increasing the current intensity from 25 to 400 μA with a step of 25 μA via an A365 stimulus isolator (WPI, USA). Responses were amplified using a Model 1800 amplifier (A-M Systems, USA) and were digitized and recorded to a personal computer using ADC/DAC NI USB-6211

(National Instruments, USA) and WinWCP v5.2.4 software (University of Strathclyde, UK). The electrophysiological data were analyzed using the Clampfit 10.2 program (Axon Instruments, USA). For each fEPSP, the slope of the rising phase at a level of 20–80% of the peak amplitude was measured. Fiber volleys (FVs) were measured from the baseline to the peak. To estimate the efficacy of synaptic excitatory neurotransmission, the relationship between the fEPSP and FV amplitudes was determined for each slice. The maximum rise slope of the curve (fEPSP amplitude vs. FV amplitude) was calculated by fitting it with a sigmoidal Gompertz function (Eq. (1)):

$$y = ae^{-e(-k(x-x_c))} \quad (1)$$

where

$a$  is an asymptote of the maximum fEPSP amplitude;

$e$  is Euler's number ( $e = 2.71828\dots$ );

$k$  is a positive number that determines the slope of the curve;

$x_c$  is the FV amplitude at which the maximum slope of the curve is observed.

The maximum slope was calculated as  $ak/e$ . To measure the paired-pulse ratio (PPR), paired pulses were delivered once every 20 s at interstimulus intervals of 10, 20, 30, 40, 50, 60, 70, 80, 90, 100, 150, 200, 300, 400, and 500 ms (Postnikova, Amakhin, Trofimova, Smolensky, & Zaitsev, 2019). The PPR was calculated as the quotient of the second and first fEPSP amplitude for each interval.

### 2.5. LTP of excitatory synaptic transmission

LTP was examined in 21–28-d-old Wistar rats. The strength of the stimulus pulse was adjusted to elicit an fEPSP with an amplitude of 40–50% of maximal and was then fixed at this level. The slices received one paired stimulation pulse (rectangular: duration, 0.1 ms; interstimulus interval, 50 ms) every 20 s. Once stable baselines were obtained for 20 min (baseline), LTP was induced via theta-burst stimulation (TBS) (five bursts of five 100-Hz pulses, with a 200-ms interval between the bursts, applied five times every 10 s; 125 pulses in total). LTP induction was then followed by 40-min recordings of fEPSPs. The strength of excitatory synaptic responses was assessed by measuring the slope (20–80%) of the fEPSP rising phase. The size of the LTP was defined as the average slope of fEPSP 30–40 min after the induction of LTP normalized to the mean magnitude of the slope for the 10-min period immediately before the delivery of the TBS (Postnikova et al., 2019).

### 2.6. Immunohistochemistry

Rats (20-d-old, eight in each group) were decapitated, and the tissue blocks from one of the hemispheres of their brains were fixed in 10% formalin in phosphate-buffered saline (PBS, pH 7.4), cryoprotected in 20% sucrose in PBS, frozen, and then sectioned at the coronal plane. The analysis of the blocks of brain tissue started at the level of 3.30 mm from Bregma (Paxinos & Watson, 2006). In total, 10 of 10-μm-thick hippocampal slices were used per animal, and the distance between the analyzed slices was 40 μm. The slices were double stained for synaptopodin (mouse monoclonal S9567 antibodies, Sigma, 1:500) and PSD95 (rabbit polyclonal ab18258 antibodies, Abcam, 1:400), a postsynaptic marker protein. The distribution of the PSD95 marker protein was analyzed to reveal possible degeneration of the dendrite system and postsynaptic terminals in the hippocampus of rats, exposed to prenatal hypoxia. The primary antibodies were diluted in 1% bovine serum albumin in PBS and visualized using a polyclonal FITC-conjugated goat secondary antibody against mouse IgG (ab6785, Abcam, 1:200) or phycoerythrin (PE)-conjugated donkey anti-rabbit IgG (ab7007, Abcam, 1:200). Rat hepatic tissue was used as a negative control. For excitation of PE and FITC, a 488 nm wavelength He/Ar laser was used,

with the emission of PE being detected at 652–690 nm and FITC at a wavelength of 496–537 nm. The majority of immunostained synaptopodin protein formed FITC-labeled dots, with dots 1  $\mu\text{m}$  in diameter corresponding to dendritic spines. The number of synaptopodin-positive spines was calculated in a  $100 \times 100 \mu\text{m}$  area, which included both the stratum radiatum and stratum moleculare (referred to hereafter as the strata radiatum/moleculare) in CA1 of the dorsal hippocampus, using the Videotest: Master Morphology 4.2 program (VideoTest, Russia) For each animal, the mean number of spines was calculated (10 slices per animal, 1 area of interest per slide). The data obtained in the hypoxia-exposed animals were compared with those of age-matched controls using an unpaired two-tailed Mann–Whitney  $U$  test ( $p < 0.05$ ).

## 2.7. Western blot

The other hemisphere of the same animals ( $n = 8$  in each group) was used for Western blot analysis. Dorsal hippocampal tissue (starting at 3.30 mm from Bregma) was taken for Western blot analysis. The quantities of synaptic-associated proteins involved in LTP were analyzed in the synaptosomal fraction containing the postsynaptic proteins and PSD95 were analyzed in whole tissue lysate in addition. The one-step synaptosomal fraction preparation procedure was based on a previous method (Phillips et al., 2001), modified later (Louneva et al., 2008). Briefly, for each sample, 0.2 g of hippocampal tissue was homogenized in a sucrose solution (320 mM sucrose, 0.1 mM  $\text{CaCl}_2$ , and 1 mM  $\text{MgCl}_2$ ) with a Sigma fast protease inhibitor cocktail (S8820, Sigma), brought to a final sucrose concentration of 1.25 M, overlaid with 1.0 M sucrose and 0.1 mM  $\text{CaCl}_2$ , and centrifuged at 20,000g for 12 h at 4 °C. The synaptosomal fraction was collected from a band at the 1.25/1.0 M sucrose interface. The synaptosomal fraction was further fractionated to separate pre- and postsynaptic material using a method described previously (Louneva et al., 2008). Briefly, the synaptosomes were pelleted at 20,000 g and then solubilized in 20 mM Tris-HCl, pH 6.0, 1% Triton X-100, 0.1 mM  $\text{CaCl}_2$ , incubated on ice for 60 min, and centrifuged at 20,000g. The pellet containing the pre- and postsynaptic membranes was solubilized in 20 mM Tris-HCl, pH 8.0, 1% Triton X-100, 0.1 mM  $\text{CaCl}_2$ , incubated on ice for 30 min, and centrifuged at 20,000g. The resulting supernatant contained the presynaptic fraction, and the pellet contained the postsynaptic fraction. The rat hepatic tissue was used as a negative control. The total amount of proteins in the sample was determined according to the Bradford protocol (Bradford, 1976). The proteins of interest were analyzed in the supernatant by electrophoresis in 12% polyacrylamide gels in the presence of sodium dodecyl sulfate, followed by immunoblotting on polyvinylidene difluoride membranes. The membranes were incubated overnight at 4 °C in the primary antibodies on 50 mM Tris-HCl, pH 7.4, with 150 mM NaCl, 0.05% Tween 20, and 5% dry nonfat milk. Primary antibodies for the proteins of interest were used: synaptopodin (mouse monoclonal S9567, Sigma, 1:1000), PSD95 (rabbit polyclonal ab18258, Abcam, 1:1000), GluN2A (NMDAR2A, rabbit polyclonal ab16646, Abcam, 1:1000), and GluN2B (NMDAR2B, rabbit polyclonal ab65783, Abcam, 1:1000). The actin protein in the same samples was analyzed using anti-actin primary antibodies (rabbit polyclonal A5060, Sigma, 1:5000). Immunoreactivity was detected using horseradish peroxidase-coupled goat anti-mouse (ab97265, Abcam, 1:5000) or goat anti-rabbit (ab6721, Abcam, 1:5000) secondary IgG and visualized using an Optiblot ECL Ultra Detect Kit (1.2 pg–2 ng) (Abcam, ab133409). The relative intensity of the immunoreactive bands on the membranes was quantified by computer-assisted densitometric measurements using Image Studio, Version 4.0.21 (LI-COR Biosciences, USA). The ratio of the intensity of the bands corresponding to the protein of interest to actin (housekeeping protein) was calculated for each sample, and the data on the hypoxia-exposed animals were compared with those of age-matched controls.

## 2.8. Open field test

The motor activity of the rats (20–28 d after birth) was assessed as the number of crossed squares in an open field test. The open field in this study was a rectangular arena of  $45 \times 45 \text{ cm}$  and with walls 13 cm high. The floor of the chamber was covered by a thick plexiglass plate and lined with 25 squares ( $9 \times 9 \text{ cm}$ ). The rat was placed in the center of the field, and the number of crossed squares was counted for 1 min. The floor of the chamber was wiped with a 50% ethanol solution after each animal. The same experimental scheme was employed for testing the control rats ( $n = 39$ ) and the rats subjected to prenatal hypoxia ( $n = 36$ ).

## 2.9. Novel object recognition test

For the analysis of the hippocampus-related cognitive functions, the novel object recognition (NOR) test was chosen (Cohen & Stackman, 2015). The NOR test, being a simple behavioral analysis of memory which based mainly on the inherent rodent exploratory behavior, has become a widely used model for studying memory disruptions in animals (Antunes & Biala, 2012; Benetti et al., 2009; Ennaceur & Delacour, 1988). The NOR test stands out from other tests because it does not require external motivation – reward or punishment, and it can be completed in a very short time (Ennaceur & Delacour, 1988; Silvers, Harrod, Mactutus, & Booze, 2007). To compare short- (STM) and long-term memory (LTM) of the control rats ( $n = 39$ ) and the rats subjected to prenatal hypoxia ( $n = 36$ ) a modification of the novel object recognition test was used. At the beginning of the trial, the experimental animal was placed in a  $45 \times 45 \text{ cm}$  box, with nontransparent 13-cm high walls for 5 min adaptation in the absence of any specific behavioral stimuli. Two hours after the adaptation to the experimental arena, during the training session, the animal was presented with two novel objects (object 1 and object 2) and left to explore these objects for 5 min.

After each training session, the animal was returned to its home cage. A period of 10 min was used to test STM, and periods of 60 min and 24 h were employed to test LTM. In the training sessions, after these periods, the animal was removed from its home case and placed in the arena in which the two objects were located. In these testing sessions, which lasted 5 min each, one of the objects (object 2) was replaced with a novel object (object 3 for testing STM, and objects 4 and 5 for LTM). Object 1 was familiar to the rats, as this remained unchanged throughout subsequent tests. For each animal, the time (T) spent in tactile or olfactory contact with each object was recorded. The preference index (PI) was calculated as the ratio of the amount of time spent exploring one of the two objects in the training phase (object 1 or 2) or the novel object (i.e., object 3) in the test phase as compared with the total time spent exploring both objects. Thus,  $PI_1$  or  $PI_2 = T_1$  or  $T_2 / (T_1 + T_2) \times 100\%$  in the training session and  $PI_3 = T_1$  or  $T_3 / (T_1 + T_3) \times 100\%$  in the test phase (Wang et al., 2007).

All the objects were made of thick glass. The objects and the experimental arena were wiped with a 50% solution of ethyl alcohol after each presentation.

## 2.10. Statistical analysis

All numerical values were expressed as the mean  $\pm$  the standard error of the mean (SEM), and all error bars on graphs represent the SEM. The numbers of slices (for electrophysiological experiments) are given in brackets. The statistical significance of the LTP data was determined using unpaired Student's  $t$ -tests for independent samples. In the analysis of animal behavior, a repeated measures analysis of variance (ANOVA), with Fisher's post hoc test was used to identify differences between the motor activity of the normal and hypoxic rats. A  $t$ -test or Mann–Whitney  $U$  test was employed to identify differences between the PI of the novel and familiar objects. All statistical analyses

were performed using Origin Pro 8 (OriginLab Co., Northampton, MA, USA) and Statistica 8.0 (StatSoft Inc., Tulsa, OK, USA), SPSS Statistics 17.0 (SPSS Inc., Chicago, IL, USA).

### 3. Results

#### 3.1. Basal synaptic transmission and LTP were attenuated in the hippocampal CA1 region after prenatal hypoxia

Long-term synaptic plasticity in the hippocampus is commonly considered as the cellular base of memory (Milner et al., 1998). Therefore, we investigated whether synaptic plasticity in the CA1 hippocampal area was affected in rats subjected to prenatal hypoxia. Before examining synaptic plasticity, we compared basal synaptic transmission and I/O relationships in the control rats and rats exposed to prenatal hypoxia. To quantify the strength of CA3–CA1 synaptic transmission, we measured presynaptic FV amplitudes, which primarily reflect the number of CA3 axons that fire an action potential, and fEPSP slopes, which mainly reflect activation of postsynaptic AMPA receptors. Field responses were evoked by electrical stimuli of varying intensities (25–400  $\mu$ A) applied using a twisted nichrome electrode placed in the stratum radiatum at the CA1–CA2 border. The amplitudes and slopes of the fEPSPs did not differ in the controls versus the rats exposed to hypoxia (repeated measures ANOVA, amplitude:  $F_{15; 1155} = 0.19$ ,  $p = 0.99$ , Fig. 1A; slope:  $F_{15; 975} = 0.92$ ,  $p = 0.54$ , Fig. 1B). In contrast, the FVs in the hypoxic rats were significantly higher than those of the control rats (repeated measures ANOVA,  $F_{15; 1095} = 32$ ,  $p < 0.001$ , Fig. 1C).

The amplitudes of the fEPSPs were plotted against the FV amplitudes to yield an I/O relation for CA3–CA1 synapses. The I/O relations

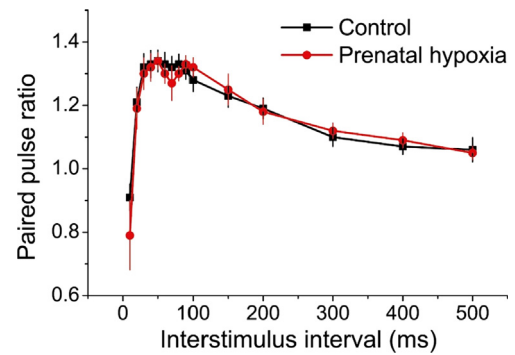


Fig. 2. Paired-pulse ratio across different inter-stimulus intervals (10–500 ms) is normal in the CA1 region of rats after prenatal hypoxia.

constructed from individual experiments were well fitted with a non-linear sigmoidal function (Fig. 1D). The slopes of these fits (I/O slopes) reflected the composite cellular transfer function between presynaptic action potential-evoked glutamate release and postsynaptic membrane responses. Therefore, the maximum I/O slope may be considered as a measure of synaptic strength. These slopes were significantly reduced in the hypoxic rats, pointing to a decrease in basal synaptic transmission functions (Fig. 1E).

To determine whether prenatal hypoxia altered presynaptic function, we examined the PPR, a transient form of presynaptic plasticity in which the second of two closely spaced stimuli elicits enhanced transmitter release. Pairs of presynaptic fiber stimulation pulses delivered at interpulse intervals of 20, 30, 40, 50, 60, 70, 80, 90, 100, 150, 200, 300, 400, and 500 ms evoked nearly identical PPRs in the slices obtained

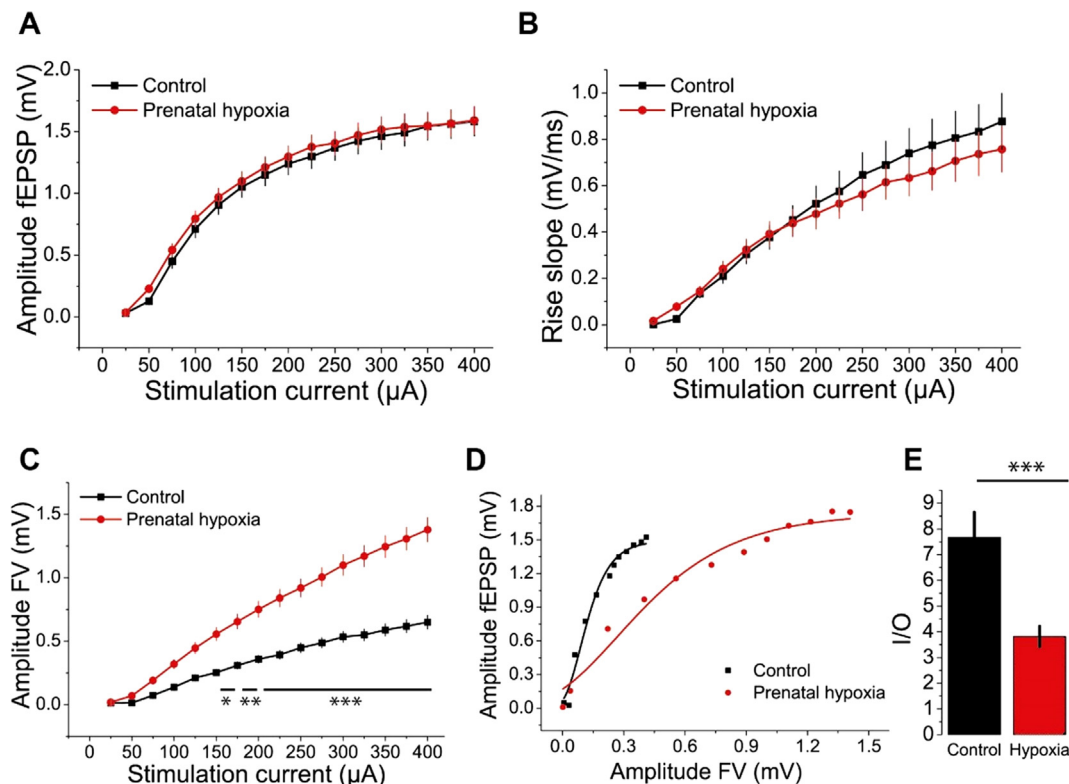
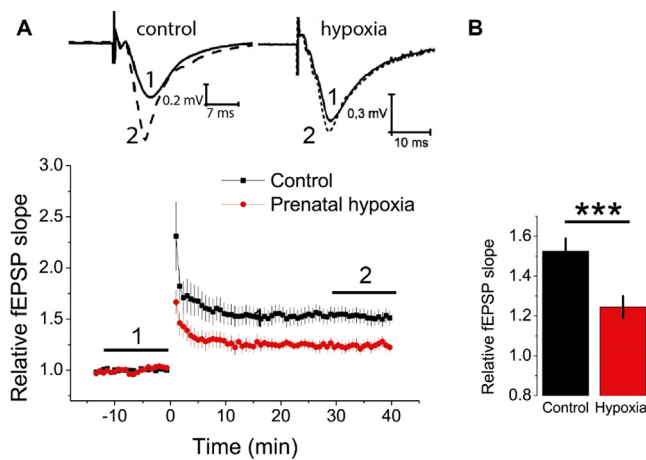


Fig. 1. Dynamics of changes in the amplitudes and rise slope of fEPSP (A, B) and presynaptic fiber volley (C) in the control group (black curve) and in the animals after prenatal hypoxia on E14 (red curve) in response to the increasing intensity of electrical stimulation of afferent fibers. (D) Representative examples of the I/O relations constructed from individual experiments relating the amplitude of the presynaptic fiber volley to the amplitude of fEPSP at various stimulus intensities (20–200  $\mu$ A) in the CA1 region of rats and fitted with Eq. (1). (E) The summary bar graph showing average maximal slopes of I/O relations between the amplitude of the presynaptic fiber volley and the amplitude of fEPSP at various stimulus intensities in the CA1 region; \* $p < 0.05$ ; \*\* $p < 0.01$ ; \*\*\* $p < 0.001$ . (For interpretation of the references to colour in this figure legend, the reader is referred to the web version of this article.)



**Fig. 3.** Long-term potentiation is attenuated in the CA1 region of the hippocampus in hypoxic rats. (A) Diagram showing the normalized slope of fEPSP in control (black) and hypoxic (red) rats before and after TBS. The inset (above) shows the examples of fEPSP before induction (1) and 40 min after TBS (2). (B) Diagram illustrating differences in LTP value between control and hypoxic groups. \*\*\* $p < 0.001$ . (For interpretation of the references to colour in this figure legend, the reader is referred to the web version of this article.)

from the controls and rats exposed to prenatal hypoxia (repeated measures ANOVA,  $F_{14;196} = 0.85$ ,  $p = 0.62$ , Fig. 2). These results suggested that presynaptic glutamate release at the CA3–CA1 synapses remained normal after prenatal hypoxia treatment.

TBS of afferent fibers resulted in robust LTP in the control rats as assessed 30–40 min after induction ( $1.51 \pm 0.06$ ,  $n = 37$  slices from 16 rats), whereas LTP was significantly reduced in the experimental rats subjected to prenatal hypoxia ( $1.24 \pm 0.05$ ,  $n = 21$  slices from 10 rats; unpaired  $t$ -tests = 3.92,  $p < 0.01$ , Fig. 3). These results demonstrated that prenatal hypoxia significantly impaired long-term synaptic plasticity at CA3–CA1 excitatory synapses in rats.

To determine the locus of LTP induction, we compared the PPR of the fEPSP amplitude before (baseline) and after induction of LTP (Fig. 4). The absence of changes in the PPR is thought to indicate a postsynaptic locus of LTP induction and the insertion of additional AMPAR into postsynaptic membrane. A change in the PPR indicates a presynaptic locus, which results in altered neurotransmitter release probability (Ivanov & Zaitsev, 2017; Zaitsev & Anwyl, 2012; Zucker & Regehr, 2002). In the present study, the PPR did not change after TBS in the control rats (pre-TBS:  $1.38 \pm 0.02$ , post-TBS:  $1.35 \pm 0.03$ ,  $n = 36$ ; paired  $t$ -test = 0.77,  $p = 0.44$ ) or in the rats subjected to prenatal hypoxia (pre-TBS:  $1.27 \pm 0.03$ , post-TBS:  $1.28 \pm 0.04$ ,  $n = 18$ ; paired  $t$ -test = 0.13,  $p = 0.90$ ). These results suggested that LTP was postsynaptically expressed both in the control and prenatal hypoxia groups

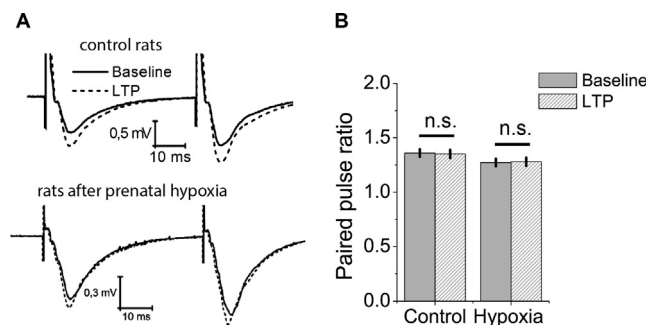


**Fig. 4.** The ratio of fEPSP amplitudes before and after the TBS. (A) Representative examples of fEPSP responses before induction (baseline) and 40 min after induction of plasticity (LTP) in CA1 from the control and hypoxic rats. (B) Diagram showing that the PPR before and after the TBS in different groups.

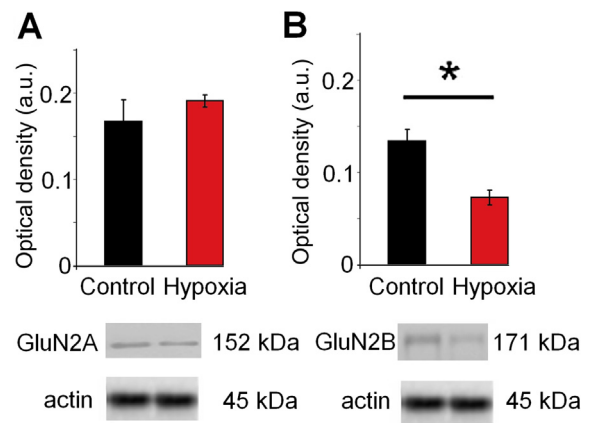


**Fig. 5.** Effects of prenatal hypoxia on the expression of NMDA receptor subunits in the hippocampus of 20 days old male rats. Western blot analysis of GluN2A (A) and GluN2B (B) subunits of NMDA receptor expression in the hippocampus tissue of control ( $n = 8$ ) and hypoxic ( $n = 8$ ) rats. The ratio of the protein of interest to actin band optical density was counted in each tissue sample. \*Difference with the control at  $p < 0.05$  (unpaired two-tailed Mann–Whitney  $U$  test).

of rats.

### 3.2. Prenatal hypoxia exposure affected the subunit composition of NMDARs in the hippocampus

As the induction of long-term synaptic plasticity in hippocampal synapses depends on the activity of NMDARs, weakening of LTP may be due to impaired expression of NMDARs or changes in their subunit composition. To test this assumption, we measured the expression level of GluN2A and GluN2B subunits of NMDARs in the dorsal hippocampus using a Western blot analysis. The results revealed a two-fold decrease in the level of the GluN2B subunit in the experimental group as compared with that in the control (Fig. 5, Mann–Whitney  $U$  test = 4.9,  $p < 0.01$ ). The expression level of the GluN2A subunit was unchanged (Fig. 5, Mann–Whitney  $U$  test = 30.0,  $p = 0.24$ ). This finding pointed to an increase in the ratio of GluN2A/GluN2B NMDA subunits in the hippocampus of young rats exposed to prenatal hypoxia on E14 as compared with that in the control animals.

### 3.3. The number of synaptopodin-positive dendritic spines decreased in the hippocampus following prenatal hypoxia

Recently, we demonstrated a significant reduction in the quantity of synaptopodin-positive dendritic spines in the neocortex and hippocampus of adult rats exposed to prenatal hypoxia on E14 (Vasilev et al., 2016; Zhuravin, Dubrovskaya, Vasilev, Tumanova, & Nalivaeva, 2011). Synaptopodin is a specific marker of labile mushroom spines (Deller et al., 2003), which play an essential role in neuronal network plasticity (Asanuma et al., 2005; Okubo-Suzuki, Okada, Sekiguchi, & Inokuchi, 2008). Therefore, in the present study, we tested whether 20-d-old rats would also show decreased numbers of synaptopodin-positive dendritic spines in the CA1 area of the hippocampus. For this purpose, using the immunofluorescence method, we counted the number of synaptopodin-positive clusters in the strata radiatum/moleculare.

To confirm the synaptic location of synaptopodin, some slices were double stained for synaptopodin and a postsynaptic marker protein, PSD95. The results revealed that all synaptopodin clusters were colocalized with PSD95-positive spots (Fig. 6A), confirming that the synaptopodin-positive specks likely corresponded to dendritic spines. The density of synaptopodin-positive specks was decreased in the strata radiatum/moleculare of the dorsal hippocampus of the rats exposed to prenatal hypoxia. In the rats exposed to prenatal hypoxia, the number

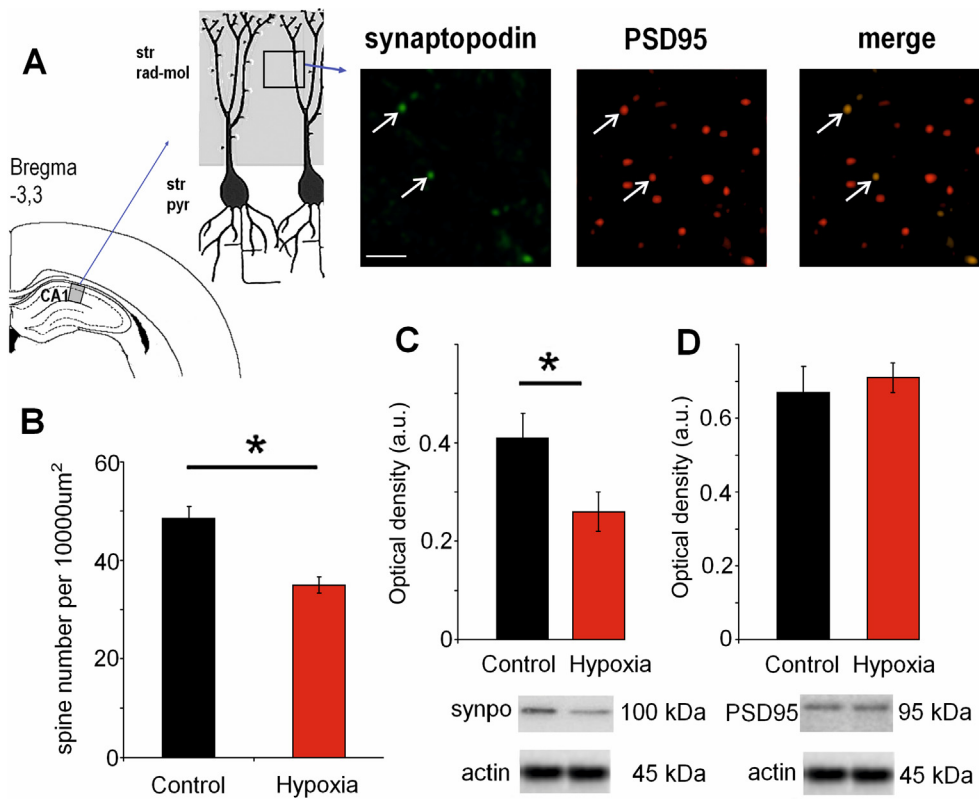


**Fig. 6.** The distribution (A-B) and level of expression of actin-associated protein synaptopodin (C) and PSD95 (D) in the dorsal hippocampus of rats. (A) Distribution of an actin-associated protein synaptopodin (green) and postsynaptic protein PSD95 (red) in stratum radiatum of the dorsal hippocampus in control rat. White arrows indicate synaptopodin-positive dendritic spines. Scale bar = 10  $\mu$ m. (B) The diagram, showing the mean density of synaptopodin-positive dendritic spines in the hippocampus of control and hypoxic rats. (C) Western blot analysis of synaptopodin (synpo) (C) and PSD95 (D) expression in the hippocampus tissue of control (n = 8) and hypoxic (n = 8) rats. The ratio of the protein of interest to actin band optical density was counted in each tissue sample. Note, that prenatal hypoxia specifically decreased the expression of the synaptopodin protein, as well as the number of dendritic spines, where this protein is localized but not the expression of PSD95. \*Difference with the control at  $p < 0.05$  (unpaired two-tailed Mann-Whitney U test). (For interpretation of the references to colour in this figure legend, the reader is referred to the web version of this article.)

of synaptopodin-positive dendritic spines was only 73% of the control level (Mann-Whitney U test = 12.6,  $p = 0.03$ ).

CA1 pyramidal cell death or degeneration of their dendrite systems could explain the changes in the number of labile synaptopodin-positive spines in rat hippocampus. To determine whether decreased expression of PSD95 accounted for the degeneration of the dendrite system and postsynaptic spines in the hippocampus of the hypoxic rats, the expression levels of PSD95 protein was estimated in brain tissue lysate with Western blot analysis. We found no difference PSD95/actin ratio between control ( $0.62 \pm 0.06$ ) and hypoxic animals ( $0.70 \pm 0.08$ ; Mann-Whitney U test = 28.4,  $p = 0.10$ ) suggesting no significant changes in the total amount of synapses. Next, we estimated synaptopodin and the PSD95 protein level in a PSD-containing synaptosomal fraction of the dorsal hippocampus. The data revealed that prenatal hypoxia decreased the synaptopodin protein level in the dorsal hippocampus, with a reduction of 36% as compared with that in the control (Fig. 6C, Mann-Whitney U test = 9.8,  $p = 0.02$ ). In contrast, there were no differences in the expression level of the postsynaptic marker PSD95 protein in the control and hypoxic rat groups (Fig. 6D, Mann-Whitney U test = 27.1,  $p = 0.14$ ).

Taken together, these results indicated that prenatal hypoxia specifically decreased the expression of the synaptopodin protein, as well as the number of dendritic spines, where this protein is localized but did not lead to degeneration of the dendrite system.

### 3.4. Prenatal hypoxia produced learning deficits in young rats

Because cognitive functions may be impaired in animals with hyperactivity due to lack of attention (Dellu-Hagedorn, 2006; Lange, Reichl, Lange, Tucha, & Tucha, 2010; Leo et al., 2018; Sontag, Tucha, Walitza, & Lange, 2010), we first investigated the motor activity of normal and hypoxic rats in an open field test. The motor activity was assessed by the number of crossed squares in the open field arena. The hypoxic rats exhibited reduced motor activity as compared with that of the control animals from 21 to 24 d after birth (Fig. 7A). To check

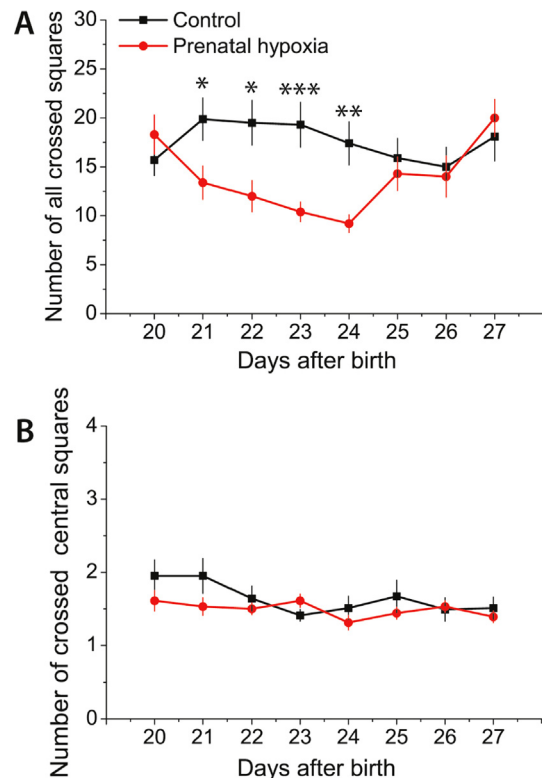


**Fig. 7.** The level of motor activity in the open field of control (n = 39) and hypoxic (n = 36) rats. Data are shown as mean  $\pm$  SEM. (A) The number of all crossed squares. Repeated measures ANOVA,  $F_{1,73} = 13.2$ ,  $p < 0.001$  following the Fisher post hoc test (stars marked statistically significant differences between control and hypoxic groups \* $p \leq 0.05$ , \*\* $p \leq 0.01$ , \*\*\* $p < 0.001$ ). (B) The number of crossed central squares. Repeated measures ANOVA,  $F_{1,73} = 2.0$ ,  $p = 0.20$ .

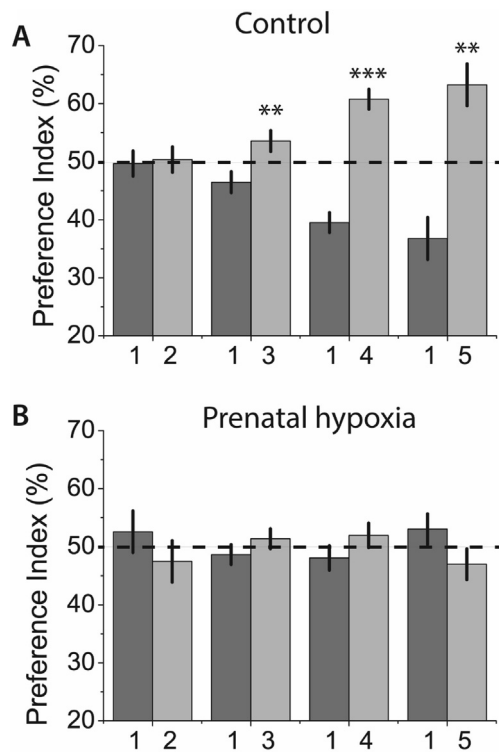


**Fig. 8.** The diagrams showing PIs in control (A,  $n = 39$ ) and hypoxic (B,  $n = 36$ ) rats in the Novel object recognition test. The horizontal line marks the hypothetical 50-% value. Paired  $t$ -test: \*\* $p \leq 0.01$ ; \*\*\* $p \leq 0.001$ . Numbers of objects are shown under the columns: training (objects 1 and 2); STM testing 10 min after training (objects 1 and 3); LTM testing 60 min after training (objects 1 and 4); LTM testing next day (objects 1 and 5).

whether the decrease in motor activity in the open field in hypoxic rats depends on a decrease in their activity in the center of the field, which could indicate an increase in anxiety of these animals (Allende-Castro et al., 2012; Smolensky et al., 2019), we investigated this parameter and found that it does not differ in control and hypoxic (Fig. 7B). Therefore, our data allow to exclude hyperactivity and increased anxiety in hypoxic rats.

The novel object recognition test was used to compare the hippocampus-related cognitive functions (Antunes & Biala, 2012; Cohen & Stackman, 2015) of rats in the control and hypoxic groups. There were no between-group differences in the total exploratory time of both objects during the training or testing sessions (control:  $6.0 \pm 0.2$  s; hypoxic rats:  $6.0 \pm 0.4$  s; Mann-Whitney  $U$  test = 204.5,  $p = 0.92$ ). The animals in both groups showed no preference for either of the two objects during the training presentation (control:  $PI_1 = 50 \pm 2\%$  for object 1;  $PI_2 = 50 \pm 2\%$  for object 2,  $n = 36$ , paired  $t$ -test = 0.2,  $p = 0.87$ ; hypoxic rats:  $PI_1 = 53 \pm 4\%$ ;  $PI_2 = 47 \pm 4\%$ ,  $n = 39$ ,  $t = 0.7$ ,  $p = 0.48$ , Fig. 8).

During the test sessions, STM (10 min after the training session) and LTM (1 h and 24 h after the training session) were evaluated. In the STM test, the control animals examined the novel object (object 3) for a longer period than the familiar object (object 1). Therefore,  $PI_3$  was larger than  $PI_1$  ( $54 \pm 2\%$  vs.  $46 \pm 2\%$ ; paired  $t$ -test = 2.9,  $p = 0.005$ ). In the LTM test 1 h later, they explored the new object (object 4) for a longer period than the familiar object ( $PI_4 = 60 \pm 2\%$  vs.  $PI_1 = 40 \pm 2\%$ ,  $t = 5.7$ ,  $p < 0.001$ ). The next day, they showed a preference for the new object again (object 5) ( $PI_5 = 63 \pm 4\%$  vs.  $PI_1 = 37 \pm 4\%$ ,  $t = 3.7$ ,  $p < 0.01$ , Fig. 8). In contrast, the rats exposed to prenatal hypoxia did not exhibit any preference for the novel objects. Ten minutes after the training session, the PIs were the same for the familiar object (object 1:  $PI_1 = 48 \pm 2\%$ ) and the new object (object 3:  $PI_3 = 52 \pm 2\%$ , paired  $t$ -test = 0.4,  $p = 0.66$ ). In the LTM

test 1 h later, the rats showed the same PIs for object 1 ( $48 \pm 2\%$ ) and object 4 ( $52 \pm 2\%$ , paired  $t$ -test = -0.9,  $p = 0.36$ ). The next day, PI5 was  $47 \pm 4\%$  for the new object (object 5) and  $53 \pm 4\%$  for the familiar object (object 1) (paired  $t$ -test = 1.1,  $p = 0.27$ ).

#### 4. Discussion

In the present study, we investigated whether prenatal hypoxia on E14 affected synaptic properties in the hippocampus and hippocampal-related cognitive functions in young rats. The prenatally stressed rats exhibited significantly disturbed basal synaptic transmission in CA-CA1 synapses, in addition to a decreased level of NMDA-dependent LTP, an altered subunit composition of NMDARs in the hippocampus, and a reduced number of synaptopodin-positive dendritic spines. All these changes resulted in learning deficits, as uncovered in a novel object recognition test. Other studies using different hypoxia models also demonstrated that prenatal hypoxia often resulted in memory deficit. For example, the deficits of recognition memory in NOR test (Cunha-Rodrigues, Balduci, Tenorio, & Barradas, 2018), reduced spatial exploration and deficit in habituation memory in open field and elevated plus maze tests (Sab et al., 2013) were shown for rats in prenatal hypoxia-ischemia model. Adult rats with prior in utero hypobaric hypoxia exhibited significant learning difficulties in both acquisition of a water maze spatial learning task and recall of a passive avoidance paradigm (Foley, Murphy, & Regan, 2005). Although the exact mechanisms underlying the effect of prenatal hypoxia on learning deficits in young rats remain unclear, many authors have suggested that damaged cognitive functions caused by prenatal hypoxia may lead to impaired neurotransmitter circuits and synaptic plasticity (Barradas et al., 2016; Cai et al., 1999; Chepkova et al., 1995; Cunha-Rodrigues et al., 2018; Herlenius & Lagercrantz, 2004; McClendon et al., 2017; Wei et al., 2016). Our electrophysiological experiments on hippocampal brain slices from prenatally stressed rats revealed some specific characteristics of synaptic dysfunction. First, we observed reduced basal synaptic transmission, as shown by a decrease in the I/O slope at the CA3-CA1 synapses. Such disturbance may arise from a reduction in the following: (i) the amount of glutamate released from each bouton due to a decrease in the probability of release and/or the vesicular content of glutamate; (ii) the density of CA1 synapses associated with each CA3 axon collateral; or (iii) postsynaptic sensitivity to glutamate, mediated by decreased function and/or density of AMPA receptors because amplitudes of fEPSP primarily reflect AMPA receptor activation. In our study, we tested some of these possible mechanisms.

In the present study, the PPR was the same in the control and prenatally hypoxic rats. The PPR is related to the probability of transmitter release (Zucker & Regehr, 2002). Thus, we suggest that prenatal hypoxia did not significantly affect the probability of transmitter release and other presynaptic functions. However, prenatal hypoxia most likely modified postsynaptic mechanisms, as demonstrated by altered postsynaptic induction of LTP, decreased density of synaptopodin-positive dendritic spines, and disturbance of the subunit composition of NMDARs.

In the present study, the rats in the prenatal hypoxia group exhibited a two-fold decrease in long-term synaptic potentiation at CA3-CA1 excitatory synapses, which is agreement with previously published data in hypoxic model (Chepkova et al., 1995). As TBS-induced LTP is an NMDAR-dependent phenomenon (Postnikova et al., 2017; Postnikova et al., 2019), this finding may point to disturbances in the expression of NMDARs. To determine whether the reduced synaptic plasticity was associated with disturbances in NMDAR gene expression, we measured the protein levels of NMDAR subunits in the hippocampus. NMDARs in the hippocampus are heterotetrameric assemblies of two GluN1 subunits and two modulatory GluN2 subunits. GluN2A and GluN2B subunits are most common in CA1 neurons and define the properties of NMDARs (Kohr, 2006). We found a two-fold decrease in the protein level of the GluN2B subunit in the hypoxic group as

compared with that in the control, suggesting that the subunit compositions of these hippocampal receptors were changed in the rats subjected to prenatal hypoxia. We investigated the expression of these receptor subunits in the early stage (i.e., the third week) of the postnatal development period, when a switch in NMDAR composition is typically observed (Sheng, Cummings, Roldan, Jan, & Jan, 1994; Williams, Russell, Shen, & Molinoff, 1993). The previous results revealed that GluN2B expression was predominant in the early stages of postnatal development. In contrast, the proportion of GluN2A-NMDARs is predominant in adult hippocampus. Thus, we conclude that exposure to prenatal hypoxia significantly affected the development of the glutamatergic mediatory system. We do not know how long these changes in receptor expression persist and whether full compensation occurs as they mature. Probably, the magnitude and duration of such disturbances depends on the model used. A decrease in the expression levels of mRNA and protein of GluN1, GluN2A, and GluN2B subunits of NMDA receptors was observed on P42 in a model of prenatal hypoxia in which the pregnant rats were treated with hypoxia (10.5% oxygen) from gestational day 4 to 21 (Wei et al., 2016). However, no decrease in GluN2B subunit expression was found in male rats on P45 using prenatal hypoxia-ischemia model (Cunha-Rodrigues et al., 2018).

Previous studies also showed that changes in the subunit composition of NMDARs significantly affected the properties of synaptic transmission and long term-plasticity (Miwa, Fukaya, Watabe, Watanabe, & Manabe, 2008; Yashiro & Philpot, 2008). For example, recombinant NMDARs containing GluN2B subunits elicited more robust and prolonged currents than GluN2A-containing NMDARs (Vicini et al., 1998). As compared with GluN2B-containing NMDARs, GluN2A-containing NMDARs exhibited a higher probability of channel opening and faster kinetics (Erreger, Dravid, Banke, Wyllie, & Traynelis, 2005), as well as providing EPSCs with more rapid decay kinetics (Amakhin et al., 2017). Some studies suggested that GluN2A-containing NMDARs preferentially induced LTP and that GluN2B-containing NMDARs were responsible for LTD (Bartlett et al., 2007; Moulton & Harvey, 2011). However, other authors showed that the role of both GluN2A- and GluN2B-containing NMDARs in synaptic plasticity was to mediate calcium influx for LTP or LTD induction, depending on the parameters of the stimulation protocols (Fox, Russell, Wang, & Christie, 2006). In this study, we used a relatively mild stimulation paradigm (TBS protocol, which likely activated mainly GluN2B-containing NMDARs as compared to high-frequency stimulation paradigms (Erreger et al., 2005). Therefore, the significant reduction in GluN2B-containing NMDARs may result in a decrease in LTP values. Similar changes in the NMDAR subunit composition and reductions in LTP were found in maternally stressed mice (Son et al., 2006) and early-life stressed mice (Lesuis, Lucassen, & Krugers, 2019).

Another possible mechanism of LTP alteration, especially of its late phase, which is resulting in impairments of memory and learning, is the decrease in the number of synaptopodin-positive spines. Synaptopodin is an actin-associated protein and is highly expressed in the spines of pyramidal neurons, where it is associated with the postsynaptic density (Mundel et al., 1997). Previous research provided convincing evidence that dendritic spines determined the character of neuronal interactions and that they were the primary substrate of plasticity (Martin, Barad, & Kandel, 2000; Segal, 2010; Zhang et al., 2013; Zito, Scheuss, Knott, Hill, & Svoboda, 2009). Synaptopodin knockout mice lacked any spine apparatus, which was accompanied by a reduction in hippocampal LTP (Deller et al., 2003). Although overexpression of synaptopodin did not affect the size and number of dendritic spines in unstimulated neurons, it maintained neural activity-dependent enlargement of dendritic spines in hippocampal neurons (Okubo-Suzuki et al., 2008). Furthermore, STM and LTM were correlated with the number of synaptopodin-positive dendritic spines in the cerebral cortex (Vasilev et al., 2016). In the present study, learning deficits and alterations in both STM and LTM were found in the young rats.

The significant decrease in the density of synaptopodin-positive

dendritic spines may be due to the death of pyramidal neurons in the CA1 zone of the hippocampus, the apical dendrites of which possesses spines. In the case of cell death, a combined decrease in the expression of synaptopodin and PSD95 would be expected. However, we did not detect any changes in the expression of the postsynaptic protein PSD95 in the rats exposed to prenatal hypoxia, which is against assumption about the death of pyramidal neurons in the CA1 zone. The decrease in the density of synaptopodin-positive dendritic spines may be attributed to disturbed afferentation in the CA1 field, similar to changes observed in the dentate gyrus in a previous study (Deller et al., 2006). We suggest that the changes in the number of the labile synaptopodin-positive spines observed in the rat hippocampus are provoked by some specific molecular mechanism regulating spine formation rather than by CA1 pyramidal cell death and degeneration of their dendrite systems.

In summary, our study revealed that prenatal hypoxia had a marked effect on hippocampal synaptic plasticity and learning in young rats. Although the precise mechanisms underlying these hippocampal disturbances will require further investigations, the present results point to alterations in the functioning of the glutamatergic system, specifically a decrease in the number of GluN2B-containing NMDA receptors. The latter may be a clinically plausible molecular target for preventing the cognitive consequences of prenatal hypoxia. Another possible mechanism of impairments in learning and memory in hypoxic animals may be decreased expression of synaptopodin, with this decrease adversely affecting the spine apparatus and altering LTP expression.

## Funding

This work was supported by the Russian Foundation for Basic Sciences (projects 17-00-00408 and 19-015-00232) and within the state assignment of Ministry of Science and Higher Education of the Russian Federation (AAAA-A18-118012290373-7).

## References

- Allende-Castro, C., Espina-Marchant, P., Bustamante, D., Rojas-Mancilla, E., Neira, T., Gutierrez-Hernandez, M. A., ... Herrera-Marschitz, M. (2012). Further studies on the hypothesis of PARP-1 inhibition as a strategy for lessening the long-term effects produced by perinatal asphyxia: Effects of nicotinamide and theophylline on PARP-1 activity in brain and peripheral tissue: Nicotinamide and theophylline on PARP-1 activity. *Neurotoxicity Research*, 22(1), 79–90. <https://doi.org/10.1007/s12640-012-9310-2>.
- Amakhin, D. V., Malkin, S. L., Ergina, J. L., Kryukov, K. A., Veniaminova, E. A., Zubareva, O. E., & Zaitsev, A. V. (2017). Alterations in properties of glutamatergic transmission in the temporal cortex and hippocampus following pilocarpine-induced acute seizures in Wistar rats. *Frontiers in Cellular Neuroscience*, 11, 264. <https://doi.org/10.3389/fncel.2017.00264>.
- Antunes, M., & Biala, G. (2012). The novel object recognition memory: Neurobiology, test procedure, and its modifications. *Cognitive Processing*, 13(2), 93–110. <https://doi.org/10.1007/s10339-011-0430-z>.
- Asanuma, K., Kim, K., Oh, J., Giardino, L., Chabanis, S., Faul, C., ... Mundel, P. (2005). Synaptopodin regulates the actin-bundling activity of alpha-actinin in an isoform-specific manner. *Journal of Clinical Investigation*, 115(5), 1188–1198. <https://doi.org/10.1172/JCI23371>.
- Babenko, O., Kovalchuk, I., & Metz, G. A. (2015). Stress-induced perinatal and transgenerational epigenetic programming of brain development and mental health. *Neuroscience & Biobehavioral Reviews*, 48, 70–91. <https://doi.org/10.1016/j.neubiorev.2014.11.013>.
- Barradas, P. C., Savignon, T., Manhaes, A. C., Tenorio, F., da Costa, A. P., Cunha-Rodrigues, M. C., & Vaillant, J. (2016). Prenatal systemic hypoxia-ischemia and oligodendroglia loss in cerebellum. *Advances in Experimental Medicine and Biology*, 949, 333–345. [https://doi.org/10.1007/978-3-319-40764-7\\_16](https://doi.org/10.1007/978-3-319-40764-7_16).
- Bartlett, T. E., Bannister, N. J., Collett, V. J., Dargan, S. L., Massey, P. V., Bortolotto, Z. A., ... Lodge, D. (2007). Differential roles of NR2A and NR2B-containing NMDA receptors in LTP and LTD in the CA1 region of two-week old rat hippocampus. *Neuropharmacology*, 52(1), 60–70. <https://doi.org/10.1016/j.neuropharm.2006.07.013>.
- Benetti, F., Mello, P. B., Bonini, J. S., Monteiro, S., Cammarota, M., & Izquierdo, I. (2009). Early postnatal maternal deprivation in rats induces memory deficits in adult life that can be reversed by donepezil and galantamine. *International Journal of Developmental Neuroscience*, 27(1), 59–64. <https://doi.org/10.1016/j.ijdevneu.2008.09.200>.
- Bird, C. M., & Burgess, N. (2008). The hippocampus and memory: Insights from spatial processing. *Nature Reviews Neuroscience*, 9(3), 182–194. <https://doi.org/10.1038/nrn2335>.
- Bradford, M. M. (1976). A rapid and sensitive method for the quantitation of microgram

- quantities of protein utilizing the principle of protein-dye binding. *Analytical Biochemistry*, 72, 248–254.
- Cai, Z., Xiao, F., Lee, B., Paul, I. A., & Rhodes, P. G. (1999). Prenatal hypoxia-ischemia alters expression and activity of nitric oxide synthase in the young rat brain and causes learning deficits. *Brain Research Bulletin*, 49(5), 359–365.
- Chepkova, A. N., Trofimov, S. S., Smolnikova, N. I., Gudasheva, T. A., Ostrovskaya, R. U., & Skrebtskii, V. G. (1995). Impaired plasticity of hippocampal synaptic transmission in rats exposed to prenatal hypoxia is normalized by treatment with nootropic dipeptides. *Bulletin of Experimental Biology and Medicine*, 120(6), 1208–1210. <https://doi.org/10.1007/bf02445573>.
- Cohen, S. J., & Stackman, R. W., Jr. (2015). Assessing rodent hippocampal involvement in the novel object recognition task. A review. *Behavioural Brain Research*, 285, 105–117. <https://doi.org/10.1016/j.bbr.2014.08.002>.
- Collingridge, G. L., Isaac, J. T., & Wang, Y. T. (2004). Receptor trafficking and synaptic plasticity. *Nature Reviews Neuroscience*, 5(12), 952–962. <https://doi.org/10.1038/nrn1556>.
- Cunha-Rodrigues, M. C., Balduci, C., Tenorio, F., & Barradas, P. C. (2018). GABA function may be related to the impairment of learning and memory caused by systemic prenatal hypoxia-ischemia. *Neurobiology of Learning and Memory*, 149, 20–27. <https://doi.org/10.1016/j.nlm.2018.01.004>.
- Deller, T., Bas Orth, C., Vlachos, A., Merten, T., Del Turco, D., Dehn, D., ... Frotscher, M. (2006). Plasticity of synaptotodin and the spine apparatus organelle in the rat fascia dentata following entorhinal cortex lesion. *The Journal of Comparative Neurology*, 499(3), 471–484. <https://doi.org/10.1002/cne.21103>.
- Deller, T., Korte, M., Chabanis, S., Drakew, A., Schwegler, H., Stefani, G. G., ... Mundel, P. (2003). Synaptotodin-deficient mice lack a spine apparatus and show deficits in synaptic plasticity. *Proceedings of the National Academy of Sciences of the United States of America*, 100(18), 10494–10499. <https://doi.org/10.1073/pnas.1832384100>.
- Dellu-Hagedorn, F. (2006). Relationship between impulsivity, hyperactivity and working memory: A differential analysis in the rat. *Behavioral and Brain Functions*, 2, 10. <https://doi.org/10.1186/1744-9081-2-10>.
- Desplats, P. A. (2015). Perinatal programming of neurodevelopment: Epigenetic mechanisms and the prenatal shaping of the brain. *Advances in Neurobiology*, 10, 335–361. [https://doi.org/10.1007/978-1-4939-1372-5\\_16](https://doi.org/10.1007/978-1-4939-1372-5_16).
- Ennaceur, A., & Delacour, J. (1988). A new one-trial test for neurobiological studies of memory in rats. 1: Behavioral data. *Behavioural Brain Research*, 31(1), 47–59.
- Erreger, K., Dravid, S. M., Banke, T. G., Wyllie, D. J., & Traynelis, S. F. (2005). Subunit-specific gating controls rat NR1/NR2A and NR1/NR2B NMDA channel kinetics and synaptic signalling profiles. *Journal of Physiology*, 563(Pt 2), 345–358. <https://doi.org/10.1113/jphysiol.2004.080028>.
- Foley, A. G., Murphy, K. J., & Regan, C. M. (2005). Complex-environment rearing prevents prenatal hypoxia-induced deficits in hippocampal cellular mechanisms necessary for memory consolidation in the adult Wistar rat. *Journal of Neuroscience Research*, 82(2), 245–254. <https://doi.org/10.1002/jnr.20641>.
- Fox, C. J., Russell, K. L., Wang, Y. T., & Christie, B. R. (2006). Contribution of NR2A and NR2B NMDA subunits to bidirectional synaptic plasticity in the hippocampus in vivo. *Hippocampus*, 16(11), 907–915. <https://doi.org/10.1002/hipo.20230>.
- Herlenius, E., & Lagercrantz, H. (2004). Development of neurotransmitter systems during critical periods. *Experimental Neurology*, 190(Suppl 1), S8–S21. <https://doi.org/10.1016/j.expneurol.2004.03.027>.
- Ivanov, A. D., & Zaitsev, A. V. (2017). NMDAR-independent hippocampal long-term depression impairment after status epilepticus in a lithium-pilocarpine model of temporal lobe epilepsy. *Synapse (New York, N. Y.)*. <https://doi.org/10.1002/syn.21982>.
- Kim, J. J., & Diamond, D. M. (2002). The stressed hippocampus, synaptic plasticity and lost memories. *Nature Reviews Neuroscience*, 3(6), 453–462. <https://doi.org/10.1038/nrn849>.
- Kohr, G. (2006). NMDA receptor function: Subunit composition versus spatial distribution. *Cell and Tissue Research*, 326(2), 439–446. <https://doi.org/10.1007/s00441-006-0273-6>.
- Lange, K. W., Reichl, S., Lange, K. M., Tucha, L., & Tucha, O. (2010). The history of attention deficit hyperactivity disorder. *Attention Deficit and Hyperactivity Disorders*, 2(4), 241–255. <https://doi.org/10.1007/s12402-010-0045-8>.
- Leo, D., Sukhanov, I., Zoratto, F., Illiano, P., Caffino, L., Sanna, F., ... Gainetdinov, R. R. (2018). Pronounced hyperactivity, cognitive dysfunctions, and BDNF dysregulation in dopamine transporter knock-out rats. *Journal of Neuroscience*, 38(8), 1959–1972. <https://doi.org/10.1523/JNEUROSCI.1931-17.2018>.
- Lesuis, S. L., Lucassen, P. J., & Krugers, H. J. (2019). Early life stress impairs fear memory and synaptic plasticity; a potential role for GluN2B. *Neuropharmacology*, 149, 195–203. <https://doi.org/10.1016/j.neuropharm.2019.01.010>.
- Louneva, N., Cohen, J. W., Han, L. Y., Talbot, K., Wilson, R. S., Bennett, D. A., ... Arnold, S. E. (2008). Caspase-3 is enriched in postsynaptic densities and increased in Alzheimer's disease. *American Journal of Pathology*, 173(5), 1488–1495. <https://doi.org/10.2353/ajpath.2008.080434>.
- Martin, K. C., Barad, M., & Kandel, E. R. (2000). Local protein synthesis and its role in synapse-specific plasticity. *Current Opinion in Neurobiology*, 10(5), 587–592.
- McClendon, E., Shaver, D. C., Degener-O'Brien, K., Gong, X., Nguyen, T., Hoerder-Suabedissen, A., ... Back, S. A. (2017). Transient hypoxemia chronically disrupts maturation of preterm fetal ovine subplate neuron arborization and activity. *Journal of Neuroscience*, 37(49), 11912–11929. <https://doi.org/10.1523/JNEUROSCI.2396-17.2017>.
- Milner, B., Squire, L. R., & Kandel, E. R. (1998). Cognitive neuroscience and the study of memory. *Neuron*, 20(3), 445–468.
- Miwa, H., Fukaya, M., Watabe, A. M., Watanabe, M., & Manabe, T. (2008). Functional contributions of synaptically localized NR2B subunits of the NMDA receptor to synaptic transmission and long-term potentiation in the adult mouse CNS. *Journal of Physiology*, 586(10), 2539–2550. <https://doi.org/10.1113/jphysiol.2007.147652>.
- Moult, P. R., & Harvey, J. (2011). NMDA receptor subunit composition determines the polarity of leptin-induced synaptic plasticity. *Neuropharmacology*, 61(5–6), 924–936. <https://doi.org/10.1016/j.neuropharm.2011.06.021>.
- Mundel, P., Heid, H. W., Mundel, T. M., Kruger, M., Reiser, J., & Kriz, W. (1997). Synaptotodin: An actin-associated protein in telencephalic dendrites and renal podocytes. *Journal of Cell Biology*, 139(1), 193–204.
- Nalivaeva, N. N., Turner, A. J., & Zhuravin, I. A. (2018). Role of prenatal hypoxia in brain development, cognitive functions, and neurodegeneration. *Frontiers in Neuroscience*, 12, 825. <https://doi.org/10.3389/fnins.2018.00825>.
- Nyakas, C., Buwalda, B., & Luiten, P. G. (1996). Hypoxia and brain development. *Progress in Neurobiology*, 49(1), 1–51.
- Okubo-Suzuki, R., Okada, D., Sekiguchi, M., & Inokuchi, K. (2008). Synaptotodin maintains the neural activity-dependent enlargement of dendritic spines in hippocampal neurons. *Molecular and Cellular Neuroscience*, 38(2), 266–276. <https://doi.org/10.1016/j.mcn.2008.03.001>.
- Paxinos, G., & Watson, C. (2006). *The rat brain in stereotaxic coordinates*. Academic Press.
- Phillips, G. R., Huang, J. K., Wang, Y., Tanaka, H., Shapiro, L., Zhang, W., ... Colman, D. R. (2001). The presynaptic particle web: Ultrastructure, composition, dissolution, and reconstitution. *Neuron*, 32(1), 63–77.
- Plata, A., Lebedeva, A., Denisov, P., Nosova, O., Postnikova, T. Y., Pimashkin, A., ... Semyanov, A. (2018). Astrocytic atrophy following status epilepticus parallels reduced Ca<sup>2+</sup> activity and impaired synaptic plasticity in the rat hippocampus. *Frontiers in Molecular Neuroscience*, 11, 215. <https://doi.org/10.3389/fnmol.2018.00215>.
- Postnikova, T. Y., Amakhin, D. V., Trofimova, A. M., Smolensky, I. V., & Zaitsev, A. V. (2019). Changes in functional properties of rat hippocampal neurons following pentylentetrazole-induced status epilepticus. *Neuroscience*, 399, 103–116. <https://doi.org/10.1016/j.neuroscience.2018.12.029>.
- Postnikova, T. Y., Trofimova, A. M., Ergina, J. L., Zubareva, O. E., Kalemenev, S. V., & Zaitsev, A. V. (2019). Transient switching of NMDA-dependent long-term synaptic potentiation in CA3-CA1 hippocampal synapses to mGluR1-dependent potentiation after pentylentetrazole-induced acute seizures in young rats. *Cellular and Molecular Neurobiology*, 39(2), 287–300. <https://doi.org/10.1007/s10571-018-00647-3>.
- Postnikova, T. Y., Zubareva, O. E., Kovalenko, A. A., Kim, K. K., Magazanik, L. G., & Zaitsev, A. V. (2017). Status epilepticus impairs synaptic plasticity in rat hippocampus and is followed by changes in expression of NMDA receptors. *Biochemistry (Moscow)*, 82(3), 282–290. <https://doi.org/10.1134/s0006297917030063>.
- Sab, I. M., Ferraz, M. M. D., Amaral, T. A. S., Resende, A. C., Ferraz, M. R., Matsuura, C., ... Mendes-Ribeiro, A. C. (2013). Prenatal hypoxia, habituation memory and oxidative stress. *Pharmacology Biochemistry and Behavior*, 107, 24–28. <https://doi.org/10.1016/j.pbb.2013.04.004>.
- Segal, M. (2010). Dendritic spines, synaptic plasticity and neuronal survival: Activity shapes dendritic spines to enhance neuronal viability. *European Journal of Neuroscience*, 31(12), 2178–2184. <https://doi.org/10.1111/j.1460-9568.2010.02720.x>.
- Sheng, M., Cummings, J., Roldan, L. A., Jan, Y. N., & Jan, L. Y. (1994). Changing subunit composition of heteromeric NMDA receptors during development of rat cortex. *Nature*, 368(6467), 144–147. <https://doi.org/10.1038/368144a0>.
- Silvers, J. M., Harrod, S. B., Mactutus, C. F., & Booze, R. M. (2007). Automation of the novel object recognition task for use in adolescent rats. *Journal of Neuroscience Methods*, 166(1), 99–103. <https://doi.org/10.1016/j.jneumeth.2007.06.032>.
- Smolensky, I. V., Zubareva, O. E., Kalemenev, S. V., Lavrentyeva, V. V., Dyomina, A. V., Karepanov, A. A., & Zaitsev, A. V. (2019). Impairments in cognitive functions and emotional and social behaviors in a rat lithium-pilocarpine model of temporal lobe epilepsy. *Behavioural Brain Research*, 112044. <https://doi.org/10.1016/j.bbr.2019.112044>.
- Son, G. H., Geum, D., Chung, S., Kim, E. J., Jo, J. H., Kim, C. M., ... Kim, K. (2006). Maternal stress produces learning deficits associated with impairment of NMDA receptor-mediated synaptic plasticity. *Journal of Neuroscience*, 26(12), 3309–3318. <https://doi.org/10.1523/JNEUROSCI.3850-05.2006>.
- Sontag, T. A., Tucha, O., Walitz, S., & Lange, K. W. (2010). Animal models of attention deficit/hyperactivity disorder (ADHD): A critical review. *Attention Deficit and Hyperactivity Disorders*, 2(1), 1–20. <https://doi.org/10.1007/s12402-010-0019-x>.
- Vasilev, D. S., Dubrovskaya, N. M., Tumanova, N. L., & Zhuravin, I. A. (2016). Prenatal hypoxia in different periods of embryogenesis differentially affects cell migration, neuronal plasticity, and rat behavior in postnatal ontogenesis. *Frontiers in Neuroscience*, 10, 126. <https://doi.org/10.3389/fnins.2016.00126>.
- Vicini, S., Wang, J. F., Li, J. H., Zhu, W. J., Wang, Y. H., Luo, J. H., ... Grayson, D. R. (1998). Functional and pharmacological differences between recombinant N-methyl-D-aspartate receptors. *Journal of Neurophysiology*, 79(2), 555–566. <https://doi.org/10.1152/jn.1998.79.2.555>.
- Wang, D., Noda, Y., Zhou, Y., Mouri, A., Mizoguchi, H., Nitta, A., ... Nabeshima, T. (2007). The allosteric potentiation of nicotinic acetylcholine receptors by galantamine ameliorates the cognitive dysfunction in beta amyloid25–35 i.c.v.-injected mice: Involvement of dopaminergic systems. *Neuropsychopharmacology*, 32(6), 1261–1271. <https://doi.org/10.1038/sj.npp.1301256>.
- Wei, B., Li, L., He, A., Zhang, Y., Sun, M., & Xu, Z. (2016). Hippocampal NMDAR-Wnt-Catenin signaling disrupted with cognitive deficits in adolescent offspring exposed to prenatal hypoxia. *Brain Research*, 1631, 157–164. <https://doi.org/10.1016/j.brainres.2015.11.041>.
- Williams, K., Russell, S. L., Shen, Y. M., & Molinoff, P. B. (1993). Developmental switch in the expression of NMDA receptors occurs in vivo and in vitro. *Neuron*, 10(2), 267–278.
- Yashiro, K., & Philpot, B. D. (2008). Regulation of NMDA receptor subunit expression and its implications for LTD, LTP, and metaplasticity. *Neuropharmacology*, 55(7), 1081–1094. <https://doi.org/10.1016/j.neuropharm.2008.07.046>.

- Zaitsev, A. V., & Anwyl, R. (2012). Inhibition of the slow afterhyperpolarization restores the classical spike timing-dependent plasticity rule obeyed in layer 2/3 pyramidal cells of the prefrontal cortex. *Journal of Neurophysiology*, *107*(1), 205–215. <https://doi.org/10.1152/jn.00452.2011>.
- Zhang, X. L., Poschel, B., Faul, C., Upreti, C., Stanton, P. K., & Mundel, P. (2013). Essential role for synaptopodin in dendritic spine plasticity of the developing hippocampus. *Journal of Neuroscience*, *33*(30), 12510–12518. <https://doi.org/10.1523/JNEUROSCI.2983-12.2013>.
- Zhuravin, I. A., Dubrovskaya, N. M., Vasilev, D. S., Tumanova, N. L., & Nalivaeva, N. N. (2011). Epigenetic and pharmacological regulation of the amyloid-degrading enzyme neprilysin results in modulation of cognitive functions in mammals. *Doklady Biological Sciences*, *438*, 145–148. <https://doi.org/10.1134/S001249661103015X>.
- Zhuravin, I. A., Tumanova, N. L., & Vasilev, D. S. (2009). Structural changes of the hippocampus nervous tissue in rat ontogenesis after prenatal hypoxia. *Journal of Evolutionary Biochemistry and Physiology*, *45*(1), 156–158.
- Zito, K., Scheuss, V., Knott, G., Hill, T., & Svoboda, K. (2009). Rapid functional maturation of nascent dendritic spines. *Neuron*, *61*(2), 247–258. <https://doi.org/10.1016/j.neuron.2008.10.054>.
- Zucker, R. S., & Regehr, W. G. (2002). Short-term synaptic plasticity. *Annual Review of Physiology*, *64*, 355–405. <https://doi.org/10.1146/annurev.physiol.64.092501.114547>.